Control of Self-Organized Contact Instability and Patterning in Soft Elastic Films

ARTICLE *in* LANGMUIR · SEPTEMBER 2006

Impact Factor: 4.46 · DOI: 10.1021/la0600696 · Source: PubMed

Control of Self-Organized Contact Instability and Patterning in Soft Elastic Films

Manoj Gonuguntla, Ashutosh Sharma,* Rabibrata Mukherjee, and Subash A. Subramanian

Department of Chemical Engineering, Indian Institute of Technology, Kanpur-208016, India

Received January 8, 2006. In Final Form: April 20, 2006

The surface of a soft elastic film becomes unstable and forms a labyrinth pattern when a rigid flat plate is brought into adhesive contact, without application of any external pressure. These isotropic undulations have a characteristic wavelength, $\lambda \sim 3H$, where H is the film thickness. We present here technique of ordering, aligning, and modulating these micro-labyrinth structures by using a patterned stamp, by varying the stamp-film inter-surface distance, by a lateral confinement of the instability and even by a simple shear motion of a flat stamp. Many complex structures, such as an array of femto-liter beakers and doubly periodic channels, are generated from a simple stamp consisting of parallel channels. The elastic nature of the patterns allows an in-situ tuning, manipulation, and reconfiguration of the microstructures. Regardless of their precise morphology, the structures continue to have the elastic length scale, $\lambda \sim 3H$. The structures can also be made permanent as required by UV−ozone-induced oxidation of the structures. The underlying principles of the elastic contact instability presented here have the potential to develop into a new soft lithography technique—elastic contact lithography (ECL), allowing a simple, rapid and large area patterning of soft solids.

Introduction

Spontaneously formed self-organized structures and their control in thin soft films are of scientific and technological importance in confinement-induced meso-scale properties, wetting,[1] adhesion,[2−4] microfluidics,[5] and patterning applications[6−19] in optoelectronics, sensors, lab-on-a-chip devices, MEMS, etc. The surface of a soft solid film, such as cross-linked poly(dimethylsiloxane) (PDMS), becomes spontaneously rough on a short instability length scale of about three times the film thickness (independent of any other material properties!) simply by bringing it in contact with a flat rigid surface.[2,20] We show that this self-organized isotropic structure undergoes morphological transitions (pillars to labyrinth structures to cavities) merely by decreasing the distance between the stamp and the film, but the length scale on the instability remains largely unaltered, independent of the type of structures. Furthermore, we also show that these elastic patterns can be aligned, ordered and modulated by (a) pattern confinement in narrow spaces, (b) shearing motion of the stamp, and (c) use of patterned stamps. The elastic contact instability can generate a variety of complex ordered structures from the *same* stamp, thus pointing a way toward an in-situ tunable control, manipulation, and re-configuration of "structures-on-demand" achieved by a combination of these control strategies and by varying the stamp-film separation.

Thin soft films confined by the long-range forces such as the van der Waals interactions and electric fields are inherently metastable or unstable and thus readily self-organize their shapes to reduce the total energy.[1−4,13−16,20,21] The self-organizing morphological response of thin *liquid* films (such as polymer melts) and various strategies for its control for meso-patterning have been extensively studied.[1,13−16,21] This forms the basis for a host of soft lithographies such as the capillary force lithography,[11] electrostatic force lithography,[13] pattern directed dewetting,[14−16] etc. that are of special potential in the microfabrication of various structures for cell/DNA sampling, sensors, lab-on-a-chip devices, polymeric displays, optical applications, micropatterned cell-substrata,[22,23] tiny reactors for nanoparticles,[24] and PDMS-based micro-patterned adhesives.[25] It may be noted that the self-organization of thin liquid films is engendered by the long-wave instability,[1,13−16,21] the length scale of which is highly sensitive to the exact nature and decay of the confining field. However, a direct *self-organized* micro-structuring of solid films under external fields and its control have been much less studied with a few notable exceptions limited to the buckling instability of a hard metal film on soft substrates such as PDMS elastomers[10] and responsive hydrogels.[9]

* Corresponding author. E-mail: ashutos@iitk.ac.in. Phone: +91-512-2597026. Fax: +91-512-2590104.

(1) Reiter, G. *Phys. Rev. Lett.* **1992**, *68*, 75.
(2) Monch, W.; Herminghaus, S. *Europhys. Lett.* **2001**, *53*, 525.
(3) Ghatak, A.; Chaudhury, M. K.; Shenoy, V.; Sharma, A. *Phys. Rev. Lett.* **2000**, *85*, 4329.
(4) Ghatak, A.;. Chaudhury, M. K. L*angmuir* **2003**, *19*, 2621.
(5) Thorsen, T.; Roberts, R. W.; Arnold, F. H.; Quake, S. R. *Phys. Rev. Lett.* **2001**, *86*, 4163.
(6) Xia, Y.; Whitesides, G. M. *Angew. Chem., Int. Ed.* **1998**, *37*, 550.
(7) Gates, B. D.; Xu, Q.; Love, C.; Wolfe, D. B.; Whitesides, G. M. *Annu. Rev. Mater. Res.* **2004**, *34*, 339.
(8) Geissler, M.; Xia, Y. *Adv. Mater.* **2004**, *16*, 1249.
(9) Hu, Z.; Chen, Y.; Wang, C.; Zheng, Y.; Li, Y. *Nature* **1998**, *393*, 149.
(10) Bowden, N.; Brittain, S.; Evans, A. G.; Hutchinson, J. W.; Whitesides, G. M. *Nature* **1998**, *393*, 146.
(11) Suh, K. Y.; Lee, H. H. *Adv. Funct. Mater.* **2002**, *12*, 405.
(12) (a) Chou, S. Y.; Krauss, P. R.; Renstrom, P. J. *Science* **1996**, *272*, 85. (b) Khang, D.-Y.; Yoon, H.; Lee, H. H. *Adv. Mater.* **2001**, *13*, 749.
(13) Schäffer, E.; Thurn-Albrecht; T.; Russel, T. P.; Steiner, U. *Nature* **2000**, *403*, 874.
(14) Higgins, M.; Jones, R. A. L. *Nature* **2000**, *404*, 476.
(15) Kargupta, K.; Sharma, A. *Phys. Rev. Lett.* **2001**, *86*, 4536.
(16) Zhang, Z.; Wang, Z.; Xing, R.; Han, Y. *Polymer* **2003**, *44*, 3737.
(17) Xia, Y.; Kim, E.; Zhao, X.; Rogers, J. A.; Prentiss, M.; Whitesides, G. M. *Science* **1996**, *273*, 347.
(18) Seo, S.; Park, J.; Lee, H. H. *Appl. Phys. Lett.* **2005**, *86*, 133114−1.
(19) Bowden, N.; Huck, W. T. S.; Paul, K. E.; Whitesides, G. M. *Appl. Phys. Lett.* **1999**, *75*, 2557.
(20) (a) Shenoy, V.; Sharma, A. *Phys. Rev. Lett.* **2001**, *86*, 119. (b) Ru, C. Q. *J. Appl. Phys.* **2001**, *90*, 6098. (c) Hui, C.-Y.; Glassmaker, N. J.; Tang, T.; Jagota, A. *J. R. Soc. London Interface* **2004**, *1*, 35. (d) Huang, S.-Q.; Li, Q.-Y.; Feng, X.-Q.; Yu, S.-W. *Mech. Mater.* **2006**, *38*, 88.
(21) Reiter, G.; Khanna, R.; Sharma, A. *Phys. Rev. Lett.* **2000**, *85*, 1432.
(22) Beningo, K. A.; Wang, Y.-L. *Trends Cell Biol.* **2002**, *12*, 79.
(23) Lee, C. J.; Blumenkranz, M. S.; Fishman, H. A.; Bent, S. F. *Langmuir* **2004**, *20*, 4155.
(24) Barton, J. E.; Odom, T. W. *Nano Lett.* **2004**, *4*, 1525.
(25) Ghatak, A..; Mahadevan, L.; Chung, J. Y.; Chaudhury, M. K.; Shenoy, V. *Proc. R. Soc. London A* **2004**, *460*, 2725..

10.1021/la0600696 CCC: $33.50
Published on Web 07/01/2006

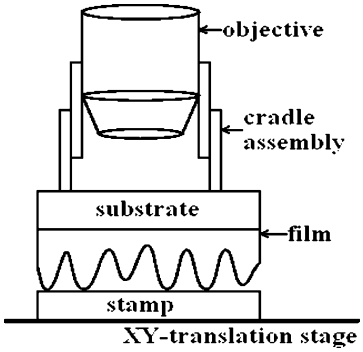

Figure 1. Schematic of the experimental setup.

We study here the morphological response of a soft (shear modulus < 10 MPa) elastomeric film when it comes in gentle contact with a rigid stamp and suggest several novel strategies for the control of the resulting short-wave pattern (wavelength ~ film thickness), which can be modulated in-situ by stamp movement. For example, using a 1D stamp consisting only of parallel grooves, we obtain distinct structural elements such as channels, arrays of femto-liter beakers, pillars, and their combinations merely by varying the inter-surface distance between the stamp and the film. This demonstrates the key strength of the process in obtaining patterns that are remarkably distinct from that on the stamp. Generation of patterns distinct from that on the stamp and their in-situ modulations cannot be easily achieved by other known lithographic techniques. We thus explore the basic scientific aspects of a potential flexible soft lithography technique based on the modulation and control of the self-organized morphology engendered by (partial) adhesion of soft elastic interfaces to a stamp.

Materials and Methods

Sylgard-184 (a two-part PDMS elastomer; Dow Chemicals, USA) consisting of oligomer and cross linking agent was used to prepare the elastic films with shear moduli of 0.1 and 1 MPa by varying the percentage of cross-linker between 5 and 10 wt %. The modulus of the films was measured by the oscillatory parallel plate method (Bohlin rheometer). Thin films of Sylgard were spin coated from its solution in *n*-heptane (HPLC grade, E. Merck) onto thoroughly cleaned quartz or silicon substrates. The thickness of the films was controlled between 500 nm to 10 μm thickness by varying the concentration of Sylgard in solvent and the RPM of spin coating. The films were subsequently cured at 120 °C for 12 h. The rms roughness of the spin cast thin films was about 1.2 nm as measured from atomic force microscope (AFM) scans. Different stamps such as flat silanized silicon wafers, microfabricated silicon structures, and even CD and DVD polycarbonate surfaces denuded of their protective coverings were used.

In some experiments, the elastic film coated on a glass substrate was directly mounted on the objective of an optical microscope (Leica; LMDM) to enable in-situ observations in relatively thicker films during the approach and retraction of the stamp as it was brought in adhesive contact proximity to the film using the focus control of the microscope. The schematic of this setup is shown in Figure 1. The glass substrate was coupled to the microscope objective with the help of a cradle, which had a fine screw for rotation and better focusing at the film surfaces. All the optical microscopy measurements were performed in the reflected light mode. The stamp was placed on the XY translation stage of the microscope which along with the focus screw could be used as a 3D positioner. In other experiments, the stamp was simply placed on the elastomer surface. The height of the structures as imaged with an AFM (PicoPlus; Molecular Imaging) measured the inter-surface distance between the film and the stamp. Prior to the AFM scanning, the patterns were preserved by the UV−ozone-induced surface hardening of silicon containing elastomer. PDMS undergoes surface oxidation under intense UV emissions (for 30 min) in the presence of oxygen to form a stiff layer of silicon oxides.[10,26] This prevented the film from relaxing even after the contactor was removed and the film could be scanned with AFM.

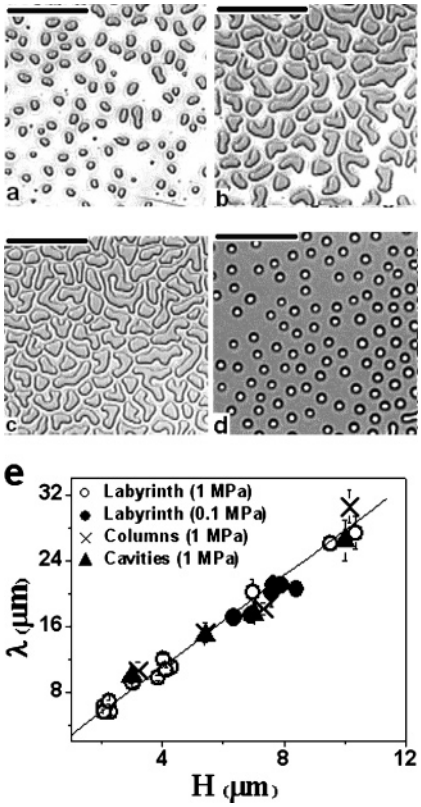

Figure 2. Optical micrographs of elastic contact instability patterns with a flat stamp during its approach and increased adhesion to a 4.58 μm thick Sylgard film (μ = 1 MPa). (a) Columns at the onset of instability, (b) elongated columns flattening to a labyrinth structure, (c) fully developed labyrinth structure, and (d) isolated circular cavities. The darker regions in all the images correspond to the film surface in contact with the stamp; scale bars = 50 μm. (e) Variation of pattern-wavelength with film thickness. Line is the best linear fit with slope = 2.77 ± 0.08.

Results and Discussions

We first present a summary of the relevant events in the evolution of the elastic contact instability when a flat stamp is brought in increasing adhesive contact with an elastic film. This brief background is required to understand the control strategies proposed later for the modulation of patterns. The patterns reported here appeared spontaneously at different distances between the film and the flat stamp and underwent morphological transitions as the separation distance varied. Three distinct classes of isotropic patterns formed by the contact instability under a flat stamp as observed in-situ by optical microscopy are shown in Figure 2a−d for a film of thickness 4.58 μm. As a flat stamp approaches the film and forms the first adhesive contact, the onset of instability results in the formation of isolated circular columns (Figure 2a). As the stamp is displaced closer toward the film, the columns become shorter with a concurrent increase in their cross-sectional area and, thus, increased contact area of the film with the stamp. The column cross-section also becomes increasingly noncircular and eventually, an isotropic labyrinth pattern of the kind shown in Figure 2, panels b and c, is formed by merger of neighboring

(26) Schnyder, B.; Lippert, T.; KÖtz, R.; Wpkaun, A.; Graubner, V.; Nuyken, O. *Surf. Science* **2003**, *532−535*, 1067.

columns. Upon further reduction of the inter-surface distance, the labyrinth pattern changes into isolated circular pits or cavities seen in Figure 2d. In a different curved contactor geometry, cavities were also seen as the precursors to the finger-like structures where the separation distance is less.[4]

The dominant wavelength (λ) of the patterns as determined by the FFT of the images is plotted as function of the film thickness (H) in Figure 1e, and the best fit shows a linear dependence of the form $\lambda = 2.77\ (\pm 0.08)\ H$. Neither a change in the shear modulus of the film by an order of magnitude nor the material of stamp (silicon wafer, quartz, and silanized silicon wafer) altered the pattern-length scale statistically significantly. Even more interesting is the observation that the wavelength of the patterns in different regimes of columns, labyrinths, and cavities remain nearly the same, except very close to the full contact and complete debonding. Thus, the precise morphology and size of the features are governed by the stamp-film separation, but the mean pattern-length scale remains rather robust regardless of the precise morphology. This feature of the elastic contact instability allows pattern generation and its in-situ transformations at a desired lateral length scale, which can only be modulated by changing the film thickness.

The above experimental observations are in agreement with the linear stability analysis and the energy minimization simulations of the contact instability, both of which predict the scaling, $\lambda = 2.96\,H$.[2−4,20,27] Earlier studies of labyrinth structures,[2] 2D finger patterns with curved flexible contactors,[3,4] and some of the dots produced by AFM scratches[28] in thin polymer films also support similar scalings.

The following simplified scaling analysis helps understand the basic physics of linear dependence of the length scale on the film thickness. Basically, the total energy of the film-stamp system is composed of two components:[3,20,27] (a) destabilizing inter-surface adhesive forces such as the van der Waals and the electrostatic and (b) stabilizing stored elastic energy penalty due to the film deformation. When the stamp comes in close proximity (<100 nm) and the inter-surface attraction exceeds a critical value, the elastic surface becomes unstable.[3,20,27] The deformation occurs on a length scale that minimizes the elastic energy. The elastic strain energy (per unit area) of the film is given by:[3,20,27] $U \sim \mu H\,(\partial v/\partial x + \partial u/\partial z)^2$, where μ is the elastic modulus, H is mean film thickness, x and z are the lateral and the normal directions, and u and v are the components of the displacement field in the x and z directions, respectively. The displacement continuity equation, $(\partial u/\partial x + \partial v/\partial z) = 0$, together with the characteristic length scales, $x \sim \lambda$, $z \sim H$, and $v \sim \delta$ (vertical amplitude of the pattern), finally give a simple scaling for the elastic stored energy due to the shear and normal deformations of the film:

$$U \sim \mu H \delta^2 (\lambda^{-1} + \lambda H^{-2})^2$$

Basically, the energy penalty is high both for very short ($\lambda \ll H$) and for very long ($\lambda \gg H$) waves, and thus the minimum elastic energy pattern (for which $\partial U/\partial \lambda = 0$) has a length scale of the order of the film thickness, $\lambda \sim H$. A detailed linear stability analysis of the governing equations provides the numerical pre-factor, $\lambda \approx 3H$.[3,20,27] Interestingly, the analysis also supports the observation that the lateral length scale at the onset of instability is independent of the elastic modulus of the film. However, the 2D nonlinear analysis[27] cannot address the issue of the precise 3D morphology of the structures that are experimentally explored here.

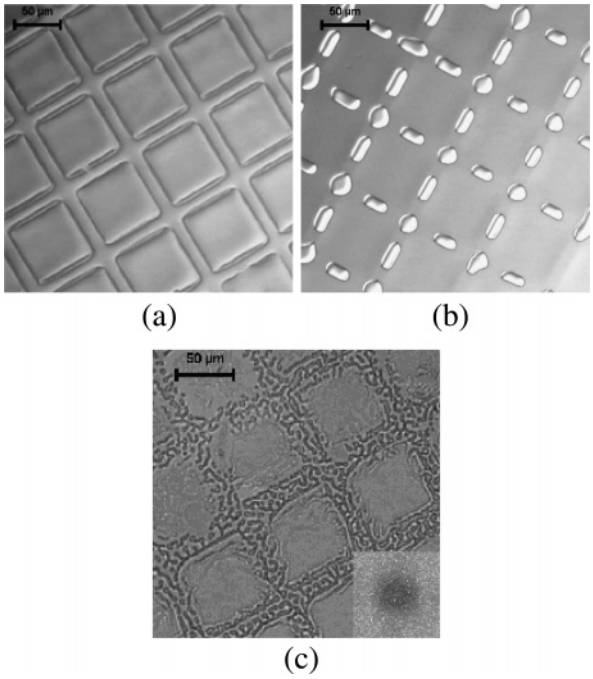

Figure 3. Optical micrographs of the elastic structures confined in 1D soft channels when a flat stamp is brought in contact with a patterned film. (a) The soft channels are 20 μm wide and the hard squares are 60 × 60 μm. (b) 1D aligned cavities (bright areas) in the soft channels of a 14.6 μm thick film. (c) 2D labyrinths in the channels of a 2.4 μm thick film. Inset in (c) is the FFT of the region where labyrinth structures are seen. Scale bars = 50 μm.

Further, 2D nonlinear simulations have shown that after the onset of the instability, the pattern length scale does not change upon further approach or retraction of the stamp because of a "pinning" of the initial structures in a local metastable state.[27] The intersurface distance thus merely controls the morphology and the width of individual features, without changing the pattern periodicity. However, previous 2D simulations[27] cannot predict the precise morphology and the morphological transitions discussed here, nor do they address the experimental pattern control and modulation strategies proposed here.

The isotropic disordered patterns witnessed under a flat stamp could be aligned and modulated in three different ways. The first strategy is the lateral confinement of the pattern in spaces smaller than the instability wavelength. The film was first patterned by placing a copper grid on its surface and exposing it to the UV−ozone treatment to produce the narrow soft channels shown in Figure 3a, which are about 60 nm lower in height than the square shaped hardened regions. When a flat silicon wafer stamp was gently pressed on this patterned film, cavities or pits confined to the soft channels emerged spontaneously as in Figure 3b. The periodicity of the cavities along a channel is 40 μm on a 14.6 μm thick film, which indeed respects the elastic instability wavelength, $\lambda \sim 3H$. Thus, the wavelength of instability persists in a confined 1D geometry of a narrow channel when its width is smaller than λ ($\sim 3H$). An identical protocol repeated on a 2.4 μm m thick film resulted in a 2D labyrinth pattern (Figure 3c), which is similar to the unconfined patterns because the channels are now much wider than λ ($\sim$7.5 μm). Basically, in this technique, the lateral confinement effects leading to 1D alignment of the structures are manifested in spaces smaller than about 3H.

Next, we explored the use of a simple patterned silicon stamp shown by the AFM image in the inset of Figure 4. A typical set

(27) Sarkar, J.; Shenoy, V.; Sharma, A. *Phys. Rev. Lett.* **2004**, *93*, 018302.
(28) Cavallini, M.; Biscarini, F.; Léon, S.; Zerbetto, F.; Bottari, G.; Leigh, D. *Science* **2003**, *299*, 531.

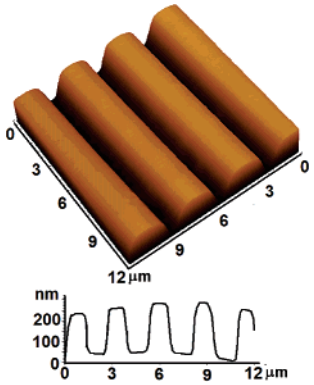

Figure 4. AFM image and the cross-sectional profile of the stamp used.

of results is shown for a stamp with protruding stripes of 200 nm heights, 1.5 μm widths, and a periodicity of 3 μm. The regions below the protrusions experience greater attraction due to their closer proximity to the stamp and become unstable first. A variety of distinct structures evolved depending on the separation distance and the ratio of the pitch of the features on the stamp and the film thickness. For a 960 nm thick film (Figure 5a−d), the pattern periodicity (3 μm) is nearly the same as the wavelength of elastic instability ($\lambda \sim 3H$). A positive replica of the stamp features (1D parallel stripes under the stamp protrusions) is thus faithfully mirrored in the elastic deformations of the film. The height of the stripe pattern (Figure 5a) created in the film is 427 ± 7.4 nm. The height of the structures thus produced is much greater than the maximum height of the stamp pattern (~200 nm), showing that the structure is not a negative replica of the stamp by imprinting**.** As the separation distance between the film and the stamp reduces, the raised ridges are slightly compressed. This leads to the spontaneous formation of a secondary 2D periodic structure in the form of bridges joining the parallel neighboring stripes. This bifurcation to the 2D instability thus results in the formation of an array of femto-liter beakers as seen in Figure 5b. The maximum height of these structures is 387 ± 6.38 nm. Interestingly, the bridges and the femto-liter beakers thus formed between the stripes also respect the periodicity of the elastic contact instability (periodicity of the "beakers" is 3.4 ± 0.2 μm which is close to $\lambda \sim 3H$). The lateral bridging, which transforms the 1D structure into a periodic 2D structure, releases the greater degree of imposed confinement, and increases the contact area between the film and the stamp. The array of tiny reactors thus formed can be employed for doing chemistry in confined spaces, including formation of ordered array of nanoparticles.[24] A further reduction of the inter-surface distance increasingly tends to produce a negative replica of the stamp as seen in Figure 5c, where the polymer ridges now shift to the spaces between the stamp protrusions. The height of ridges is 110 ± 3 nm, which indicates that these structures are now formed by the imprint of the stamp on the film. Remnants of some holes still remain, which disappear only on further compression by application of external pressure. At this point, the method becomes identical to the room-temperature imprint lithography.

On the other hand, at greater separation distance between the film and the stamp, oriented and elongated pillars (mean height of 451 ± 10.82 nm), rather than cavities, are generated as seen in Figure 5d. Thus, morphological transitions under a patterned stamp appear to mirror the corresponding changes under a flat stamp—formation of isolated cavities or beakers at smaller inter-surface distance, which change to ridges and isolated pillars at higher separation. The patterned stamp however provides a

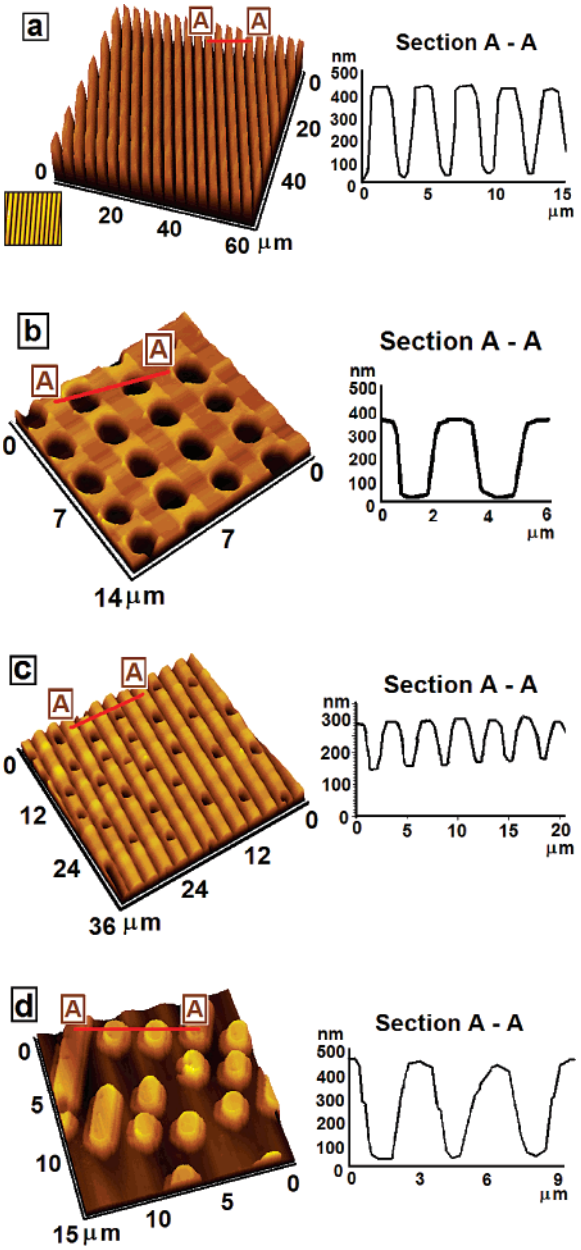

Figure 5. Modulation of elastic instability by patterned stamps. (a) Positive replica of the stamp formed by the first adhesive contact; inset shows the stamp. (b) Transition to a 2D array of femto-liter beakers by lateral bridging between the neighboring stripes at closer approach of the stamp. (c) Greater negative replication of the stamp with remnants of cavities at still closer approach. (d) Columns formed by the fragmentation of structure in panel a upon retraction of the stamp.

preferred direction to the structures, which are otherwise isotropic under a flat stamp.

The results discussed thus far correspond to the case when the stamp periodicity (~ 3 μm) is similar to the wavelength of elastic contact instability (~ 3H) in a 960 nm thick film. The role played by the stamp periodicity vis-à-vis the instability wavelength is now considered.

When the stamp-pitch is much larger or smaller than the elastic contact instability wavelength ($\lambda \sim 3H$), the positive-replica pattern shown in Figure 5a develops additional complexities due to a mismatch between the stamp pitch and the instability wavelength (Figure 6a,b). For example, Figure 6a shows the formation of two raised ridges and an intervening channel under every protrusion of the stamp when the thickness of the PDMS

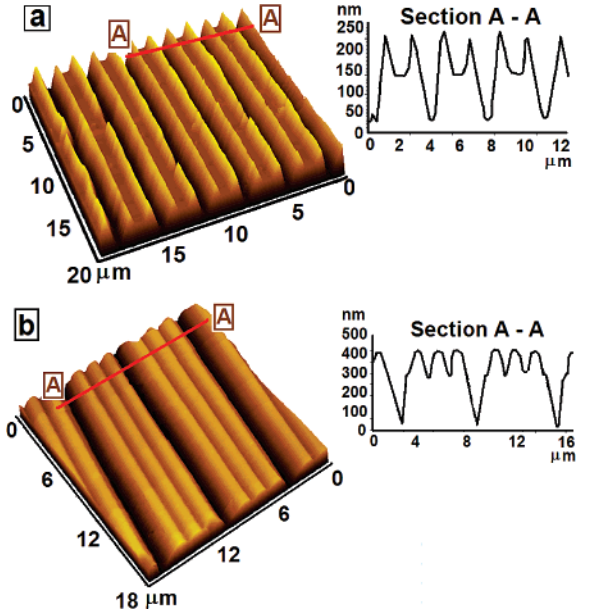

Figure 6. Self-organized structures generated when the elastic instability wavelength, $\lambda \sim 3H$, does not match with the pitch of the pattern on the stamp. (a) Two parallel ridges form under each protrusion of a stamp having wide stripes (width $\sim$ pitch/2 $\sim \lambda$). (b) Incomplete replica under a stamp with narrow stripes (width $\sim$ pitch/2 $\sim \lambda/5$) where each broad ridge, consisting of three narrower faint ridges, is separated by the contact instability wavelength, λ.

film is reduced to about 480 nm (the stamp pitch is now twice the instability wavelength for a 480 nm thick film). Thus, pattern periodicity smaller than the stamp periodicity can be engineered by reducing the film thickness. In contrast, consider the example when the elastic instability length scale is larger than the stamp-pitch as in Figure 6b (where CD stamp-pitch = 1.5 μm, width of stripe = 750 nm, film thickness 1.89 μm, wavelength $\sim$ 6 μm). In this case, every fourth stamp protrusion fails to produce a raised ridge and every ridge spans over three protrusions of the stamp. The resulting structure thus indeed attains a periodicity of the elastic contact instability, where the distance between two consecutive deep channels is $\sim$6 μm (Figure 6b). Each of the broad ridges also retains a faint imprint of the overlying stamp protrusions due to slight imprinting.

These examples further show that the structures produced by the self-organized elastic contact instability are not mere replicas of the stamp, as in the imprint lithographies. The morphology and periodicity of elastic instability patterns can thus be controlled, organized, aligned, and scaled by varying the inter-surface distance, film thickness, and pattern size of the stamp.

The patterns formed in soft elastic films by elastic contact can be formed over a large area ($\sim$ cm^2). For example, the optical micrographs of Figure 7 shows the patterns formed in a 1.2 μm thick PDMS film by bringing the patterned stamp into contact. Figure 7a corresponds to the positive replica of the stamp, and Figure 7b corresponds to the array of femto-liter beakers.

Even more complex 2D structures can also be engineered by a simple 1D patterned stamp by a repeated withdrawal, rotation, and reapplication of the stamp. This is illustrated in the examples of Figure 8a,b where the 1D stamp (CD polycarbonate stamp, pitch = 1.5 μm) was first brought into close proximity to the films and the resulting striped patterns were partially hardened by the UV−ozone treatment for a short duration ($\sim$ 5 min) to prevent their immediate relaxation. The stamp was then withdrawn, rotated, and brought back into contact with the film

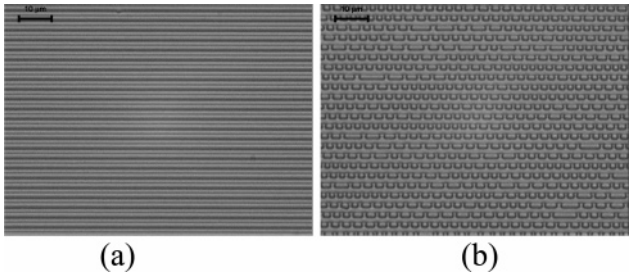

Figure 7. Optical micrographs of the large area patterns generated in Sylgard films from the stamp shown in Figure 3. (a) The positive replica of the channels. (b) The array of femto-liter beakers at closer approach. Scale bar in both images = 10 μm.

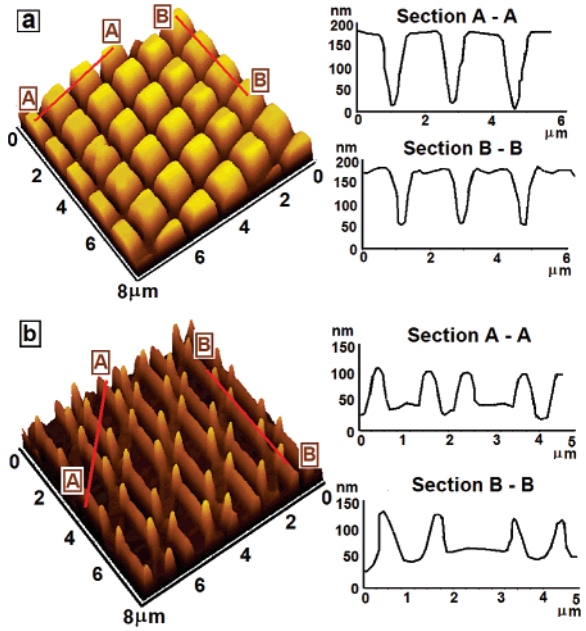

Figure 8. Pattern of complex two-dimensional alignment generated by two-step contact with intermediate partial surface hardening. (a) Patterns from a positive replica of the stamp, H = 300 nm (width $\sim$ pitch $\sim \lambda$). (b) Patterns when H is reduced to 90 nm. In panel b, the first pattern before the reapplication of stamp was a double channel structure similar to that in Figure 6a.

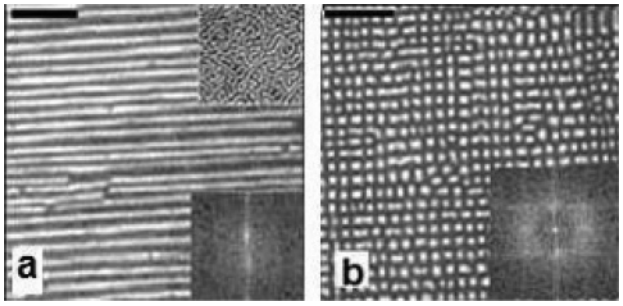

Figure 9. Shear induced alignment of the isotropic labyrinth structures under a flat stamp. (a) 1D alignment (brighter regions are channels and the upper inset shows the structure before application of shear). (b) 2D alignment. Scale bar = 15 μm, H = 740 nm.

at an angle to the initial patterns. This leads to the formation of a 2D array of pillars with a lateral dimension of 750 and 180 nm in height for a film of thickness 300 nm (Figure 8a). The stamp width in this case is nearly 3H. When the film thickness was reduced to about 90 nm (Figure 8b), the first pattern was a multi-periodic channel structure (similar to that in Figure 6a). The second contact of the stamp, oriented at 45° to the alignment of the first contact, resulted in the pattern shown in Figure 8b.

Areas measuring several centimeters squared could be patterned routinely and robustly.

Finally, we also found another novel method for aligning the 2D randomly oriented labyrinth patterns of Figure 2c into more ordered structures by a slow (∼1 mm/s) lateral movement of the flat stamp for about 3 s after it comes in contact to form a labyrinth structure (Figure 9a,b). This first shearing transforms the initial random 2D structure into a 1D anisotropic pattern aligned in the direction of shear as shown in Figure 9a. The darker regions correspond to the raised regions formed by contact of the film with the stamp. A second movement of the stamp in the direction perpendicular to the first direction results in the ordered 2D (eight nearest neighbor structure) array of cavities as shown in Figure 9b. Interestingly, the length scale of the aligned patterns still correspond to the scaling, $\lambda \sim 3H$.

Conclusions

We have shown that a variety of self-organized, ordered and reconfigurable meso-structures composed of elements such as channels, posts, and wells can be engineered in PDMS elastomeric films on the lateral length scale of ∼3*H*, by merely bringing a thin elastic film of thickness *H* in contact with a single stamp and by the movements of the stamp. Our experiments address the basic underlying principles of the elastic contact instability as well as its control and modulation by various strategies such as varying the film thickness and the stamp pitch, by the lateral and vertical movements of the stamp, and by confinement of the instability in narrow spaces smaller than 3*H*. In addition to being a potential tool for self-organized patterning directly in the solid state, the contact instability is also fundamental to the understanding of adhesion, debonding, friction, cavitation, cell mechanics, and other phenomena and applications involving confined soft interfaces. Unlike the conventional photolithography that is limited to etching of radiatively cross-linkable polymers, the elastic contact lithography can be used for any soft polymer, including hydrogels and the glassy polymers softened to the rubbery regime by heating or plasticizers. Indeed, the success of this technique in micro-patterning of hydrogels, which are an important class of materials in biological applications, will be reported elsewhere. It should be noted emphatically that the proposed patterning technique, which is based on the self-organizational principles of the elastic contact instability, is quite distinct from the top-down imprint lithographies. For example, unlike the Nano- or Micro-Imprint Lithographies[12] that aim for a permanent negative replica of the stamp topography under high pressure or temperature induced plastic deformations and viscous flow, the proposed *Elastic Contact Lithography* for a direct and flexible patterning of solids has the promise to develop into a more versatile technique. Technological developments could include further variations such as multiple layered films and coated stamps, 3D simulations of the instability with patterned stamps and the use of nano-manipulation techniques allowing controlled positioning and movement of the stamp and the film.

Acknowledgment. We thank V. Shenoy and J. Sarkar for theoretical collaborations on the contact instability, M. Ghosh for some initial optical microscopy work. and M. K. Chaudhury for illuminating discussions. The work was supported by the DST Unit on Nanoscience and Technology at IIT Kanpur.

LA0600696